A General Modeling Framework for Genome Ancestral Origins in Multiparental Populations

Chaozhi Zheng,[1] Martin P. Boer, and Fred A. van Eeuwijk
Biometris, Wageningen University and Research Centre, 6700AC Wageningen, The Netherlands

ABSTRACT The next generation of QTL (quantitative trait loci) mapping populations have been designed with multiple founders, where one to a number of generations of intercrossing are introduced prior to the inbreeding phase to increase accumulated recombinations and thus mapping resolution. Examples of such populations are Collaborative Cross (CC) in mice and Multiparent Advanced Generation Inter-Cross (MAGIC) lines in *Arabidopsis*. The genomes of the produced inbred lines are fine-grained random mosaics of the founder genomes. In this article, we present a novel framework for modeling ancestral origin processes along two homologous autosomal chromosomes from mapping populations, which is a major component in the reconstruction of the ancestral origins of each line for QTL mapping. We construct a general continuous time Markov model for ancestral origin processes, where the rate matrix is deduced from the expected densities of various types of junctions (recombination breakpoints). The model can be applied to monoecious populations with or without self-fertilizations and to dioecious populations with two separate sexes. The analytic expressions for map expansions and expected junction densities are obtained for mapping populations that have stage-wise constant mating schemes, such as CC and MAGIC. Our studies on the breeding design of MAGIC populations show that the intercross mating schemes do not matter much for large population size and that the overall expected junction density, and thus map resolution, are approximately proportional to the inverse of the number of founders.

DISSECTING the genetic architecture of complex traits is a central task in many fields such as animal breeding and crop science. There are mainly two approaches to identify the underlying quantitative trait locus/loci (QTL): QTL mapping in experimental breeding populations and association or linkage disequilibrium mapping in natural and constructed diversity panels (Cavanagh *et al.* 2008). Although association mapping among apparently unrelated individuals can greatly improve the genetic resolution of causative variants by exploring historical recombinations, it has a major disadvantage of possibly spurious associations due to unknown population structure if not accounted for appropriately (Voight and Pritchard 2005). Although well-controlled QTL mapping populations do not have such a problem, the traditional population designs such as recombinant inbred lines (RILs) and nearly isogenic lines (NILs) have low mapping resolution because of few captured recombinations and low segregation probability of QTL among only few founder lines. We use abbreviations like RIL and NIL in a rather loose way to refer to single and multiple lines as well a population as a whole.

To overcome the limitations of traditional biparental QTL mapping and association mapping, the next generations of mapping populations have been designed with multiple founders, where from one to a number of generations of intercrossing are introduced prior to the inbreeding phase to increase accumulated recombinations and thus mapping resolution. These population resources include the mouse Collaborative Cross (CC) (Churchill *et al.* 2004), the *Arabidopsis* MAGIC lines (Kover *et al.* 2009), and the *Arabidopsis* multiparent RIL (AMPRIL) (Huang *et al.* 2011).

The genome of an individual sampled from mapping populations is a random mosaic of founder origins, and it is necessary to model the ancestral origins and reconstruct them for downstream QTL mapping. For example, the reconstruction outputs such as posterior probabilities of ancestral origins at putative QTL are used as genetic predictors in the mixed model of QTL mapping (Huang *et al.* 2011). The primary goal of this article is to construct a general model of ancestral origins along

doi: 10.1534/genetics.114.163006
Manuscript received February 14, 2014; accepted for publication June 15, 2014
Supporting information is available online at http://www.genetics.org/lookup/suppl/doi:10.1534/genetics.114.163006/-/DC1.
[1]Corresponding author: Biometris, Wageningen University and Research Centre, PO Box 100, 6700AC Wageningen, The Netherlands. E-mail: chaozhi.zheng@wur.nl

two homologous chromosomes that can be applied for both traditional and next generation mapping populations.

Modeling of ancestral origins was pioneered by Haldane and Waddington (1931) in terms of two-locus diplotype (two ordered haplotypes) probabilities. Their recurrence relations were derived for 2-way RILs by selfing or sibling (brother–sister) mating and for NILs by repeated backcrossing. The closed-form solutions were given mainly for the final completely homozygous lines. Johannes and Colome-Tatche (2011) derived the two-locus diplotype probabilities for 2-way RILs by selfing. Broman (2012a) extended the approach of Haldane and Waddington (1931) to 2^n-way RILs by sibling mating and obtain only numerical recipes for calculating two-locus diplotype probabilities. The haplotype probabilities for 2^n-way RILs have been calculated by Broman (2005) and Teuscher and Broman (2007) and those for advanced inter-cross populations by Darvasi and Soller (1995), Winkler *et al.* (2003), and Broman (2012b).

For next generation mapping populations, the complexity of modeling ancestral origins along two autosomal chromosomes increases very fast with the number of founders. For example, for four-way RILs by sibling mating, there are 700 two-locus diplotype states even after accounting for various symmetries (Broman 2012a). To reduce this complexity, we assume that each founder contributes on average equally to the sample's genomes. Thus founders' identities do not matter, and we need only to model the change of ancestral origins along chromosomes.

This work builds on the theory of junctions in inbreeding (Fisher 1949, 1954). A junction is defined as a boundary point on chromosomes where two distinct ancestral origins meet, and the boundary points that occur at the same location along multiple chromosomes are counted as a single junction. Two chromosomes at a locus are identical by descent (IBD) if they have the same ancestral origins. A junction as defined on two homologous chromosomes is called internal when the two pairs of chromosome segments before and after the junction are either both IBD or both non-IBD; otherwise we call a junction external. Fisher (1949, 1954) and Bennett (1953, 1954) developed the theory of junctions for repeated sibling, selfing, and parent–offspring mating. Stam (1980) extended the theory to a finite random mating population without selfing by using recurrence relations of three-gene IBD probabilities, instead of Fisher's elaborate generation matrix for various mating types. The author obtained the expected density (per morgan) of external junctions on two chromosomes at any generation.

We generalize the Stam approach to model the ancestral origins in mapping populations. The expected densities for all junction types are systematically investigated, rather than only external junctions. The breeding population size and mating schemes may vary from one generation to the next. The number of offspring may be non-Poisson distributed or even fixed, and there may be self-fertilizations.

The closed-form expressions for the map expansion R, that is, the expected junction density on one chromosome, and the overall expected density ρ on two homologous chromosomes are derived in our approach. The latter can be used as a measure of QTL map resolution, since both simulation and analytic studies (Darvasi and Soller 1995; Weller and Soller 2004) have shown that mapping resolution is inversely proportional to ρ in traditional mapping populations. The other factors affecting map resolution include sample size and QTL effects. Thus, we may compare different QTL mapping populations or breeding designs for a particular population type, in terms of ρ.

In this article, we build a general theoretical framework for modeling ancestral original processes along two homologous autosomal chromosomes and apply it to study breeding designs of mapping populations; however, we do not use it to infer ancestral origins from observed molecular marker data. In the *Methods* section, we describe a continuous time Markov model where the rate matrix can be deduced from various expected junction densities. To evaluate the theoretical predictions for expected junction densities, various types of breeding populations with multiple stages of constant mating schemes are simulated. In addition, the breeding designs of MAGIC populations are studied, by varying the number of founders and the intercross mating schemes, from the aspect of overall expected junction density ρ and thus mapping resolution. Finally, we discuss the model assumptions such as Markov approximations and random mating schemes.

Methods

Continuous time Markov chain

Consider a diploid population founded at generation 0, and the generations are nonoverlapping. The founder population consists of L fully inbred or $L/2$ outbred founders. The mating scheme $\mathcal{M}_t$ describes how the population of size N_t at generation t produces the next generation. We first focus on two homologous autosomes from monoecious populations without selfing or equivalently dioecious populations with equal numbers of females and males. The monoecious populations with random selfing can be easily derived from non-selfing populations. See Supporting Information, Table S1 for a list of symbols used in this article.

For an individual randomly sampled from a breeding population, we model the ancestral origin processes along its two homologous chromosomes by a continuous time Markov chain, the time parameter being genetic distance along chromosomes. We assign a unique founder genome label (FGL) to the whole genome of each inbred founder or to each of the two haploid genomes of each outbred founder. The ancestral origins on two chromosomes at a single locus are represented by an ordered pair, each taking one of $L \geq 2$ possible FGLs. The ancestral origins at the leftmost locus follow the stationary distribution of the reversible Markov chain, and thus the ancestral origin process does not depend on the direction of chromosomes.

Due to the Markov assumption, it is sufficient to consider two-locus diplotypes and their marginal single-locus genotypes. We assume that founders are exchangeable so that

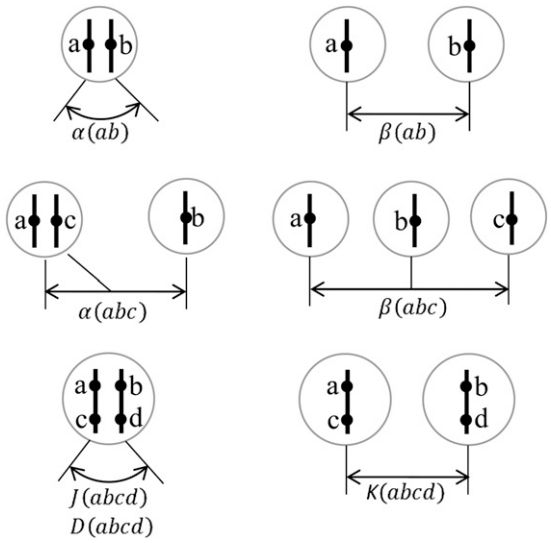

Figure 1 Quantities defined for two-, three-, and four-gene IBD configurations. Solid circles denote genes on chromosomes.

the distribution of ancestral origins does not depend on the founders' identities. As a result, single-locus genotypes and two-locus diplotypes of ancestral origins are reduced into IBD configurations, and each of the L FGLs has equal probability to be the ancestor of genes that are IBD. Let (ab), (abc), and $(abcd)$ be two-, three-, and four-gene IBD configurations, respectively. Set $a = 1$, and $b, c, \ldots$ are set in order. If the focus gene is IBD to a previous gene, the same integer label is assigned. Otherwise, one plus the maximum of the previous gene labels is assigned. We use genes and gene labels interchangeably if there are no ambiguities.

Let $D(abcd)$ be the two-locus probability of the IBD configuration $(abcd)$ given that $a(b)$ is the maternal (paternal) derived gene at one locus, $c(d)$ is the maternal (paternal) derived gene at the other locus, and haplotypes ac and bd are in a single individual (Figure 1). For the number of FGLs $L \geq 4$, there are 15 two-locus IBD configurations (Figure 2), the same as single-locus configurations in a pair of individuals (Nadot and Vayssiex 1973). In the limit that the genetic distance δ between two loci (in morgans) goes to zero, there is at most one junction between two loci. Thus $D(abcd) = 0$ as $\delta \to 0$ for the six IBD configurations (1123), (1221), (1223), (1231), (1233), and (1234) with more than one junction between two loci (Figure 2).

Since a pair of ancestral origins along two chromosomes can change or remain the same, the probabilities for the remaining nine IBD configurations are related as

$$\alpha(11) = D(1111) + D(1112) + D(1121) + D(1122), \quad (1a)$$

$$\alpha(12) = D(1212) + D(1211) + D(1222) + D(1213) + D(1232), \quad (1b)$$

where $\alpha(11)$ and $\alpha(12)$ are the marginal probabilities of IBD and non-IBD at one locus, respectively. Thus, we need only to consider the seven IBD configurations with exactly one junction between two loci, excluding the two no-junction configurations (1111) and (1212), at the limit $\delta \to 0$. The relation between two-locus IBD configurations and the seven types of junctions is shown in Figure 2.

Let $J(abcd)$ be the expected number of junctions of type $(abcd)$ per morgan, and it does not depend on the genetic distance δ. According to the theory of the continuous time Markov chain (Norris 1997), the two-locus IBD configuration probability $D(abcd) = J(abcd)\delta$ as $\delta \to 0$, and the rate matrix of ancestral origin processes is fully determined by $J(abcd)$ for the seven junction types. Since the junction densities do not depend on the direction of chromosomes, we have $J(1112) = J(1211)$ and $J(1121) = J(1222)$. In addition, the two haplotypes ac and bd are exchangeable for autosomes, and we have $J(1211) = J(1222)$ and $J(1213) = J(1232)$.

The map expansion R as a marginal expected junction density on one chromosome is given by

$$R = J(1121) + J(1122) + J(1222) + J(1232), \quad (2)$$

on the maternally derived chromosome, which is the same as the expected density, $J(1112) + J(1122) + J(1211) + J(1213)$ on the paternally derived chromosome (Figure 2), due to the symmetry between the two autosomal chromosomes. The overall expected junction density ρ on two chromosomes in a single individual is given by the sum over the seven expected junction densities. It holds that

$$\rho = 2R - J(1122) \quad (3)$$

since the junctions of type (1122) are double counted. Both R and ρ converge to $J(1122)$ as $t \to \infty$ for the case of complete inbreeding when only junctions of type (1122) exist.

In summary, under the assumption of founder symmetry the model of ancestral origin processes can be described by the initial distribution at the leftmost site of chromosomes via the one-locus non-IBD probability $\alpha(12)$ and the transition rate matrix of continuous time Markov chain that can be deduced from the three independent expected junction densities $J(1232)$, $J(1222)$, and $J(1122)$ (Norris 1997). We may replace one of the three densities by R or ρ, according to Equations 2 and 3. The recurrence relations of these expected densities are given after the next section on the non-IBD probabilities.

Recurrence relations for single-locus non-IBD probabilities

The calculation of the probabilities for four-gene IBD configurations at two loci necessitates the introduction of the probabilities for two- and three-gene IBD configurations at a single locus. In nonselfing populations, it matters whether two homologous genes are in a single individual. Let $\alpha(ab)$ be the single-locus probability of the IBD configuration (ab) given that the homologous genes a and b are in a single individual and $\beta(ab)$ be the probability given that two genes are in distinct individuals (Figure 1). There are two two-gene IBD configurations, (12) and (11), and they are related by $\alpha(11) = 1 - \alpha(12)$ and $\beta(11) = 1 - \beta(12)$.

Configurations $(abcd)$	a c b d	Chromosomes	Junction density $J(abcd)$	# junctions	# states
(1111)			N/A	0	L
(1112)			$J(1112)$	1	$L(L-1)$
(1121)		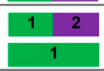	$J(1121)$	1	$L(L-1)$
(1122)		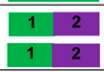	$J(1122)$	1	$L(L-1)$
(1123)			N/A	2	$L(L-1)(L-2)$
(1211)			$J(1211)$	1	$L(L-1)$
(1212)		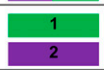	N/A	0	$L(L-1)$
(1213)		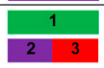	$J(1213)$	1	$L(L-1)(L-2)$
(1221)		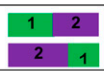	N/A	2	$L(L-1)$
(1222)		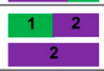	$J(1222)$	1	$L(L-1)$
(1223)			N/A	2	$L(L-1)(L-2)$
(1231)		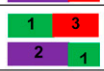	N/A	2	$L(L-1)(L-2)$
(1232)		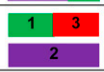	$J(1232)$	1	$L(L-1)(L-2)$
(1233)		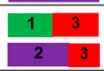	N/A	2	$L(L-1)(L-2)$
(1234)			N/A	2	$L(L-1)(L-2)(L-3)$

Figure 2 The seven types of junctions and their relations to the 15 two-locus IBD configurations. Different colors represent different ancestral chromosomes. The haplotype *ac* is maternally derived, and *bd* is paternally derived. The junction types and their densities are defined only for IBD configurations with one junction between two loci. The last column shows the number of two-locus ancestral origin states given the junction type and the number $L \geq 3$ of genome origins and in total L^4 possible states of ancestral origins at two loci. The number of junctions for the configuration (1122) is 1 because the two breakpoints are duplicated copies and thus at the same point along chromosomes.

Without selfing, two homologous genes in one individual at generation t must come from two individuals of the previous generation. The recurrence relations for the two-gene non-IBD probabilities are given by

$$\alpha_t(12) = \beta_{t-1}(12) \tag{4a}$$

$$\beta_t(12) = s_t \frac{1}{2}\alpha_{t-1}(12) + (1-s_t)\beta_{t-1}(12), \tag{4b}$$

where s_t is the coalescence probability that two genes come from a single individual of the previous generation $t-1$ given that they are in distinct individuals at generation t, and the fraction 1/2 refers to the probability that the two genes are the copies of a single gene given that they are in a single individual.

We denote by $\alpha(abc)$ the probability of the IBD configuration (abc) given that two particular homologous genes are in one individual and the third gene is in another individual and by $\beta(abc)$ the probability given that each gene is in one of three distinct individuals (Figure 1). We set two genes a and c in a single individual and gene b in another (Figure 1). This is the case in deriving the expected densities in the next section, where the configuration probability $\alpha_{t-1}(abc)$ of the previous generation $t-1$ contributes in forms of new junctions to $J_t(abcd)$ [except $J_t(1122)$] in the current generation.

Let q_t be the coalescence probability that one particular gene comes from one individual and the other two genes come from another individual of the previous generation $t-1$ given that the three genes are in distinct individuals at generation t. The recurrence relations for the three-gene non-IBD probabilities are given by

$$\alpha_t(123) = 2s_t \frac{1}{2}\alpha_{t-1}(123) + (1-2s_t)\beta_{t-1}(123) \tag{5a}$$

$$\beta_t(123) = 3q_t \frac{1}{2}\alpha_{t-1}(123) + (1-s_t-2q_t)\beta_{t-1}(123), \tag{5b}$$

where the factor 2 in Equation 5a denotes that two possible pairs of genes come from a single individual of the previous generation, and they are the pair a and b and the pair c and b, excluding the pair a and c because of nonselfing; the factor 3 in Equation 5b denotes that three possible pairs of genes come from a single individual of the previous generation. The term in parentheses $(1 - s_t - 2q_t)$ is the probability that three genes come from three distinct individuals of the previous generation $t - 1$ given that they are in distinct individuals at generation t, the probability $1 - s_t$ that one pair of genes comes from two distinct individuals minus the probability $2q_t$ that the third gene and either gene of the pair come from a single individual of the previous generation.

In addition to the two-gene IBD configurations, there is only one independent three-gene IBD configuration (*abc*) (Cockerham 1971). The probability $\alpha(122)$ is necessary in deriving the expected density $J(1222)$, and it can obtained from the relation

$$\alpha_t(1\_2) = \alpha_t(123) + \alpha_t(112) + \alpha_t(122), \tag{6}$$

where $\alpha_t(1\_2) = \alpha_t(12)$ is the marginal non-IBD probability between genes a and c. Since $\alpha_t(112) = \alpha_t(122)$ due to the symmetry between genes a and c in a single individual, we obtain $\alpha_t(122) = (\alpha_t(12) - \alpha_t(123))/2$.

Recurrence relations for expected junction densities

The accumulation of recombination events over many generations leads to genetic map expansion R, which is defined as the expected junction density (per morgan) on a randomly chosen autosomal chromosome. The derivation of the recurrence relation for R directly follows Fisher's theory of junction (Fisher 1954): a new junction is formed whenever a recombination event occurs between two homologous chromosomes that are non-IBD at the location of a crossover (Figure 3). Thus we have (MaCleod *et al.* 2005, appendix by P. Stam)

$$R_t = R_{t-1} + \alpha_{t-1}(12) = R_{t-1} + 1 - \alpha_{t-1}(11), \tag{7}$$

which shows clearly how the inbreeding slows down the map expansion.

To proceed for two homologous chromosomes, we define $K(abcd)$ as the expected junction density given that the haplotypes *ac* and *bd* are in two distinct individuals, in addition to the expected junction density $J(abcd)$ given that the two haplotypes are in a single individual (Figure 1). The contributions to junctions in the current generation come from either existing junctions at the previous generation or a new junction via a crossover event. The recurrence relations of $J(abcd)$ and $K(abcd)$ are analogous to Equations 4a and 4b for $\alpha(12)$ and $\beta(12)$, in terms of the contribution or surviving of existing junctions at the previous generation. We thus focus on the formation of a new junction.

The schematic illustrations of the recurrence relations for junction types (1232), (1222), and (1122) are shown in Figure 3. The formation of junction type (1232) involves three chromosomes: two parental chromosomes of haplotype *ac* involving in the crossover and the parental chromosome

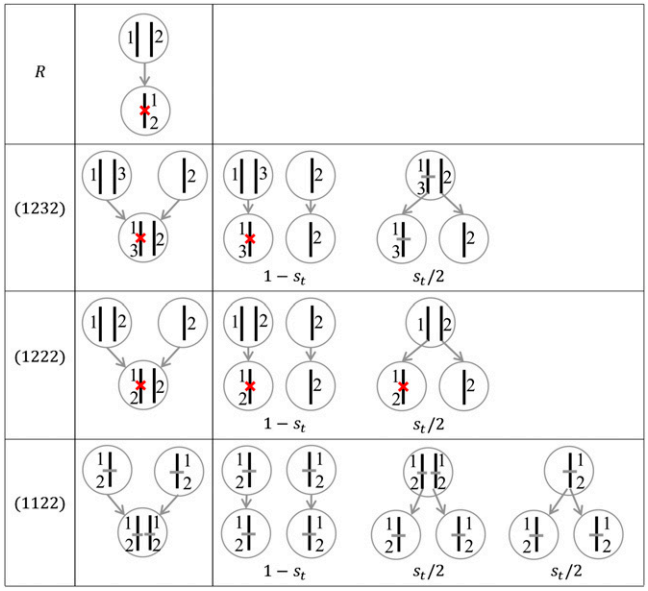

Figure 3 Schematics of the recurrence relations for the map expansion R and the expected junction densities of the types (1232), (1222), and (1122). Red x's denote the newly formed junctions in generation t, and gray horizontal bars denote the existing junctions. The center column show the junctions in a single individual of the current generation, and the right column shows the junctions in two distinct individuals of the current generation.

of haplotype *bd*. A new junction of type (1232) is formed whenever the three homologous chromosomes at the location of the crossover have the IBD configuration (123). We thus have

$$J_t(1232) = K_{t-1}(1232) + \alpha_{t-1}(123), \tag{8a}$$

$$K_t(1232) = s_t \frac{1}{2} J_{t-1}(1232) + (1 - s_t)[K_{t-1}(1232) + \alpha_{t-1}(123)], \tag{8b}$$

where the first term on the right-hand side of Equation 8b has only the contribution of the existing junctions for the scenario that the two haplotypes *ac* and *bd* come from a single individual of the previous generation.

The recurrence relations for the junctions of type (1222) can be similarly obtained. If the two haplotypes *ac* and *bd* come from two distinct individuals of the previous generation, a new junction of type (1222) is formed whenever the three homologous chromosomes at the location of the crossover have the IBD configuration (122). And if they come from a single individual of the previous generation, a new junction of type (1222) involving two homologous parent chromosomes is formed at rate $\alpha(12)$. We obtain

$$J_t(1222) = K_{t-1}(1222) + \alpha_{t-1}(122), \tag{9a}$$

$$K_t(1222) = s_t \frac{1}{2}[J_{t-1}(1222) + \alpha_{t-1}(12)] + (1 - s_t)[K_{t-1}(1222) + \alpha_{t-1}(122)], \tag{9b}$$

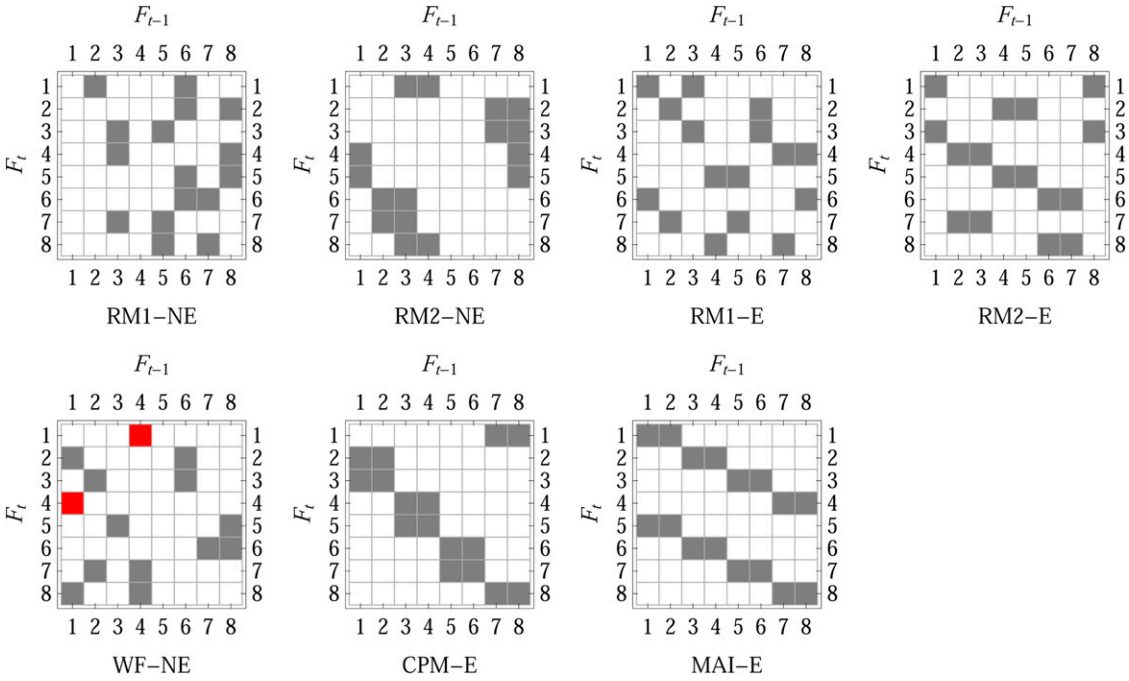

Figure 4 Intercross mating schemes represented in the format of M-matrix (Boucher and Nagylaki 1988) for a constant population of size eight. Gray entry m_{ij} denotes that individual j of the previous generation $t-1$ contributes one gamete to its offspring i, and red entries show two-gamete contributions (selfing).

which are the same as those obtained by Stam (1980) if we replace $\alpha_{t-1}(122)$ by $\alpha_{t-1}(123)$ according to Equation 6.

For continuous modeling of chromosomes, it is impossible that independent recombination events occur at exactly the same location, and thus a new junction of type (1122) can be formed only by duplicating a chromosome segment. We have

$$J_t(1122) = K_{t-1}(1122), \tag{10a}$$

$$K_t(1122) = \frac{s_t}{2}R_{t-1} + \frac{s_t}{2}J_{t-1}(1122) + (1-s_t)K_{t-1}(1122), \tag{10b}$$

where the first term on the right-hand side of Equation 10b refers to the scenario that the two haplotypes *ac* and *bd* are the copies of a single chromosome segment of the previous generation. Thus overall density ρ in Equation 3 does not depend on three-gene non-IBD probabilities according to Equation 7 and Equations 10a and 10b.

We focus on calculating the three less complicated densities R, $J(1232)$, and $J(1122)$, and they depend on the non-IBD probabilities $\alpha(12)$ and $\alpha(123)$. The basic model parameters are the two-gene coalescence probability s_t and the three-gene coalescence probability q_t, and they are determined by the population size N_{t-1} and the mating scheme $\mathcal{M}_{t-1}$ of the previous generation.

Monoecious populations with random selfing

In monoecious populations with random selfing, all the homologous genes are equivalent, and as a result it is not necessary to distinguish whether two homologous genes are in a single individual or in two distinct individuals. It is a Wright–Fisher ideal population but with variable size. We redefine s_t and q_t as unconditional coalescence probabilities regardless of two or three homologous genes being in distinct individuals or not at generation t. Thus s_t is also the probability that an individual at generation t is produced by selfing. According to Equations 4b and 5b, we have

$$\alpha_t(12) = \left(1-\frac{1}{2}s_t\right)\alpha_{t-1}(12), \tag{11a}$$

$$\alpha_t(123) = \left(1-s_t-\frac{1}{2}q_t\right)\alpha_{t-1}(123), \tag{11b}$$

where $\alpha_t(12)$ and $\beta_t(123)$ are redefined as unconditional probabilities regardless of the distribution of two or three homologous genes among individuals at generation t.

The recurrence relation for R in Equation 7 remains the same. We similarly redefine $J(1232)$ and $J(1122)$ as unconditional expected junction densities, and their recurrence relations are revised as

$$J_t(1232) = \left(1-\frac{s_t}{2}\right)J_{t-1}(1232) + (1-s_t)\alpha_{t-1}(123), \tag{12a}$$

$$J_t(1122) = \left(1-\frac{s_t}{2}\right)J_{t-1}(1122) + \frac{s_t}{2}R_{t-1}, \tag{12b}$$

according to Equations 8b and 10b.

Table 1 Coalescence probabilities for mating schemes

Mating scheme	Coalescence probability		Population size	
$\mathcal{M}_{t-1}$	s_t	q_t	N_{t-1}	N_t
Pairing	0	0	Even	$N_{t-1}/2$
Selfing	1	0	1	N_{t-1}
Sibling	1/2	0	2	N_{t-1}
Half diallel	$\frac{1}{2}\frac{N_{t-1}-2}{N_t-1}$	$s_t\left[1-\frac{1}{2}\frac{N_{t-1}-3}{N_t-2}\right]$	≥3	$\frac{N_{t-1}(N_{t-1}-1)}{2}$
Full diallel	$\frac{1}{2}\frac{2(N_{t-1}-1)-1}{N_t-1}$	$s_t\left[1-\frac{1}{2}\frac{2(N_{t-1}-1)-2}{N_t-2}\right]$	≥3	$N_{t-1}(N_{t-1}-1)$
RM1-NE	$\frac{1}{N_{t-1}}$	$s_t(1-s_t)$	≥2	≥2
RM2-NE	$\frac{1}{2(N_t-1)}+\left(1-\frac{1}{N_t-1}\right)\frac{1}{N_{t-1}}$	$\frac{1}{2(N_t-1)}\left(1-\frac{1}{N_{t-1}}\right)+\left(1-\frac{1}{N_t-1}\right)\frac{1}{N_{t-1}}$ $\times\left[1-\frac{1}{N_t-2}-\left(1-\frac{2}{N_t-2}\right)\frac{1}{N_{t-1}}\right]$	≥2	≥4 even
RM1-E	$\frac{1}{2(N_{t-1}-1)}$	s_t	≥2	N_{t-1}
RM2-E	$\frac{1}{2(N_t-1)}$	s_t	≥2 even	N_{t-1}
WF-NE	$\frac{1}{N_{t-1}}$	$s_t(1-s_t)$	≥1	≥1

The coalescence probabilities q_t are set to zero implicitly for random-selfing populations of size 1 and nonselfing populations of size 2. The coalescence probabilities for the diallel crosses are given only for monoecious populations. In the full diallel, all possible combinations of two different parents are crossed, whereas the half diallel excludes reciprocal crosses. In the coalescence probabilities s_t for RM2-NE and RM2-E, $1/(N_t-1)$ refers to the probability that the parents of the two genes come from a single mating-pair sampling (that results in two offspring), and $1/N_{t-1}$ refers to the probability that the two genes come from the same parent given that their parents come from different samplings.

Simulation of breeding populations

To evaluate the theoretical predictions of the expected junction densities, we simulate various mapping populations. Assuming that there is no natural selection, we simulate the genome ancestral origins of a breeding individual by first simulating a breeding pedigree according to the breeding design $\Omega = \{L, N_t, \mathcal{M}_t\}$ and then dropping a FGL on the pedigree. A unique FGL is assigned to the whole genome of each complete inbred founder or to the haploid gamete of each outbred founder. Each descendant gamete is specified as a list of FGL segments determined by chromosomal crossovers. In a diploid breeding population, each gamete consists of a pair of homologous chromosomes of 1 M in length. The number of crossovers between a pair of homologous chromosomes follows a Poisson distribution.

For a mapping population with the particular breeding design, the realized junction densities and IBD probabilities are saved for all individuals in any generation in each simulation replicate, and they are averaged over in total 10^4 replicates. The breeding pedigrees are fixed or vary across replicates, according to the nature of the mating scheme $\mathcal{M}_t$. Various mating schemes are used in simulating breeding pedigrees. We use *pairing* to refer to the intercross mating scheme in 2^n-way ($n \geq 1$) RILs, where individuals in parent populations are assigned to exclusive pairs, and each pair produces one offspring. The gender is alternative female and male for a dioecious population. *Selfing* and *sibling* are used to produce inbred lines at inbreeding stage.

To study the breeding design of MAGIC populations, we introduce seven intercross mating schemes. We denote by *RM1* the random mating where each sampling of two randomly chosen distinct individuals produces *one* offspring, by *RM2* the random mating where each sampling of two randomly chosen distinct individuals produces *two* offspring, and by *WF* the Wright–Fisher type random mating where each sampling of two randomly chosen individuals—distinct or not—produces one offspring. In addition, we denote by *CPM* the circular pair mating where each individual mates with its right neighbor to produce one offspring (Kimura and Crow 1963) and by *MAI* the maximum avoidance of inbreeding mating scheme (Wright 1921). We combine these mating schemes with *-NE* if each parent contributes a Poisson-distributed number of gametes to the next generation, and *-E* if each parent contributes exactly two gametes. Thus, we have five random mating schemes, RM1-NE, RM2-NE, RM1-E, RM2-E, and WF-NE, and two regular mating schemes CPM-E and MAI-E, and they are illustrated in Figure 4.

Results

Multistage breeding populations

In the definition of the recurrence relations the mating scheme $\mathcal{M}_t$ and the population size N_t are allowed to vary from one generation to the next. In that case no closed-form analytic expressions for the expected junction densities can be derived. However, experimental breeding (animal or plant) populations for QTL mapping can usually be divided into multiple stages, each stage having constant mating schemes. Thus, we may obtain closed-form solutions for multistage breeding populations by linking results via the initial conditions of each subsequent stage.

We adopt the conceptual framework of the multistage breeding designs introduced by Valdar *et al.* (2003) in the simulation studies of QTL mapping populations. The design has three stages of mixing, intercross, and inbreeding, and we use subscripts F, I, and II for them, respectively. From the model perspective, the stages are not fundamentally different, and some of them may be merged or dropped. For convenience, and in correspondence to many actual breeding populations, we choose our mixing stage to consist of one generation, where N_F founders are mated under scheme $\mathcal{M}_F$, leading to population F_1. These founders are chosen in an attempt to maximize genetic diversity.

The F_1 population is intercrossed by mating scheme $\mathcal{M}_I$ for U generations. The intercross stage $F_1 \sim F_{U+1}$ introduces accumulative recombination events and creates outbred individuals whose genomes are fine-grained mosaics of founder genomes. However, an outbreeder's genomes are heterogeneous and unique. To produce immortal lines by the paradigm of genotype once and phenotype many times, an inbreeding stage is often followed. The last intercross population F_{U+1} is inbred by mating scheme $\mathcal{M}_{II}$ for V generations. To generate nearly fully inbred lines at the last generation $g = U + V + 1$, the number V of inbreeding generations is usually ≥ 6 for selfing plants and ≥ 20 for sibling mating animals.

In the multistage framework, the breeding design can be represented by L, U, V, N_F, N_I, N_{II}, $\mathcal{M}_F$, $\mathcal{M}_I$, and $\mathcal{M}_{II}$. It holds that $N_F = L$ if founders are completely inbred that are assumed in the following for RIL and MAGIC populations. The population size N_I at the intercross stage may be fully determined by N_F if, for example, the mixing mating scheme $\mathcal{M}_F$ is diallel crosses (Table 1). The population size N_{II} at the inbreeding stage is 1 for $\mathcal{M}_{II}$ = selfing and 2 for $\mathcal{M}_{II}$ = sibling.

Constant random mating populations

The closed-form solutions of the recurrence relations in our model can be obtained for each stage of breeding populations, where the mating scheme $\mathcal{M}$ and thus the coalescence probabilities s and q are constant. The dependences of the coalescence probabilities on various mating schemes are given in Table 1. We derive explicit expressions for both random-selfing populations and nonselfing populations.

First, consider autosomes in nonselfing populations with population size $N \geq 2$. We obtain explicit expressions by solving the linear recurrence relations of order 1 in the *Methods* section. The eigenvalues of the transition matrix for the two- and three-gene non-IBD probabilities are denoted by

$$\lambda_{1,2} = \frac{1}{2}\left(1 - s \pm \sqrt{1+s^2}\right) \tag{13a}$$

$$\lambda_{3,4} = \frac{1}{2}\left(1 - 2q \pm \sqrt{1+2q+4q^2-4s-4sq+4s^2}\right), \tag{13b}$$

where $\lambda_1 > \lambda_2$, and $\lambda_3 \geq \lambda_4$. Set q and $\beta_t(123)$ to zero for $N = 2$. The explicit expressions are given in the following forms,

$$\alpha_t(12) = C_1(\lambda_1)^t + C_2(\lambda_2)^t \tag{14a}$$

$$\alpha_t(123) = C_3(\lambda_3)^t + C_4(\lambda_4)^t \tag{14b}$$

$$R_t = R_0 + \frac{C_1}{1-\lambda_1}\left[1 - (\lambda_1)^t\right] + \frac{C_2}{1-\lambda_2}\left[1 - (\lambda_2)^t\right] \tag{14c}$$

$$J_t(1122) = R_0 + \frac{C_1}{1-\lambda_1} + \frac{C_2}{1-\lambda_2} + (C_5 + C_6 t)(\lambda_1)^t + (C_7 + C_8 t)(\lambda_2)^t \tag{14d}$$

$$J_t(1232) = C_9(\lambda_1)^t + C_{10}(\lambda_2)^t + C_{11}(\lambda_3)^t + C_{12}(\lambda_4)^t, \tag{14e}$$

where the constant coefficients $C_1, \ldots, C_{12}$ are not independent, and they are determined by the eight initial conditions $\alpha_0(12)$, $\beta_0(12)$, $\alpha_0(123)$, $\beta_0(123)$, $J_0(1122)$, $K_0(1122)$, $J_0(1232)$, and $K_0(1232)$. Their expressions are given in File S1. The map expansion R_t in Equation 14c is obtained by accumulative summing of the non-IBD probability $\alpha_t(12)$ in Equation 14a. The constant term in Equation 14d is the same as the constant term in Equation 14c since $R_t = J_t(1122)$ in the case of complete inbreeding (that is, $t \to \infty$). The map expansion R_t in Equation 14c has been derived by Stam in the appendix of MaCleod *et al.* (2005).

Next consider monoecious populations with random selfing. The (largest) eigenvalues λ_1 and λ_3 for the two- and three-gene non-IBD probabilities are given by

$$\lambda_1 = 1 - \frac{s}{2}, \tag{15a}$$

$$\lambda_3 = 1 - s - \frac{1}{2}q, \tag{15b}$$

respectively. The coalescence probability q and the initial condition $\alpha_0(123)$ are set to zero for $N = 1$. From the recurrence relations of random-selfing populations in the *Methods* section, we obtain

$$\alpha_t(12) = \alpha_0(12)(\lambda_1)^t \tag{16a}$$

$$\alpha_t(123) = \alpha_0(123)(\lambda_3)^t \tag{16b}$$

$$R_t = R_0 + \frac{\alpha_0(12)}{1-\lambda_1}\left[1 - (\lambda_1)^t\right] \tag{16c}$$

$$J_t(1122) = J_0(1122)(\lambda_1)^t + R_0\left[1 - (\lambda_1)^t\right] + \frac{\alpha_0(12)}{1-\lambda_1}\left[1 - \left(1 + \frac{1-\lambda_1}{\lambda_1}t\right)(\lambda_1)^t\right] \tag{16d}$$

$$J_t(1232) = J_0(1232)(\lambda_1)^t + \alpha_0(123)\frac{2\lambda_1 - 1}{\lambda_1 - \lambda_3}\left[(\lambda_1)^t - (\lambda_3)^t\right], \tag{16e}$$

Table 2 Results for 2^n-way RILs on autosomes at the last generation $g = U + V + 1$, where $U = n - 1$ for selfing, $U = 0$ for $n = 1$ sibling, and $U = n - 2$ for $n \geq 2$ sibling

Quantity	Theoretical prediction
A. 2^n-way selfing	
$\alpha_g(12)$	$\left(\frac{1}{2}\right)^V$
$J_g(1232)$	$U\left(\frac{1}{2}\right)^V$
R_g	$U + 2\left[1 - \left(\frac{1}{2}\right)^V\right]$
ρ_g	$U\left[1 + \left(\frac{1}{2}\right)^V\right] + 2\left[1 + (V-1)\left(\frac{1}{2}\right)^V\right]$
B. 2-way sibling	
$\alpha_g(12)$	$\frac{5+\sqrt{5}}{10}(\lambda_1)^V + \frac{5-\sqrt{5}}{10}(\lambda_2)^V$
$J_g(1232)$	0
R_g	$4 - \frac{10+4\sqrt{5}}{5}(\lambda_1)^V - \frac{10-4\sqrt{5}}{5}(\lambda_2)^V$
ρ_g	$4 - \left(\frac{50+18\sqrt{5}}{25} - \frac{3+\sqrt{5}}{5}V\right)(\lambda_1)^V - \left(\frac{50-18\sqrt{5}}{25} - \frac{3-\sqrt{5}}{5}V\right)(\lambda_2)^V$
C. 2^n-way ($n \geq 2$) sibling	
$\alpha_g(12)$	$\frac{5+3\sqrt{5}}{10}(\lambda_1)^V + \frac{5-3\sqrt{5}}{10}(\lambda_2)^V$
$J_g(1232)$	$-2\left(\frac{1}{2}\right)^V + \frac{5+3\sqrt{5}}{10}(U+2)(\lambda_1)^V + \frac{5-3\sqrt{5}}{10}(U+2)(\lambda_2)^V$
R_g	$U + 6 - \frac{15+7\sqrt{5}}{5}(\lambda_1)^V - \frac{15-7\sqrt{5}}{5}(\lambda_2)^V$
ρ_g	$U + 6 - \left(\frac{75+39\sqrt{5}}{25} - \frac{5+3\sqrt{5}}{10}U - \frac{4+2\sqrt{5}}{5}V\right)(\lambda_1)^V - \left(\frac{75-39\sqrt{5}}{25} - \frac{5-3\sqrt{5}}{10}U - \frac{4-2\sqrt{5}}{5}V\right)(\lambda_2)^V$

The eigenvalues $\lambda_1 = (1+\sqrt{5})/4$ and $\lambda_2 = (1-\sqrt{5})/4$.

where $\alpha_0(12)$, $\alpha_0(123)$, R_0, $J_0(1122)$, and $J_0(1232)$ are the initial conditions, and the initial population is chosen so that $\alpha_0(12)$ and $\alpha_0(123)$ do not depend on the distribution of two or three genes among individuals. The first terms in Equations 16d and 16e refer to the surviving junctions of types (1122) and (1232), respectively.

The results for random-selfing and nonselfing populations can be unified under the following assumptions. If the population size N is large and thus s is small, the eigenvalues λ_2 and λ_4 are small, and the involved terms can be ignored. Furthermore, if the dependences of the initial conditions on the distributions of genes or haplotypes among individuals are small, the results for nonselfing populations in Equations 14a–14e are simplified to those for random selfing monoecious populations in Equations 16a–16e, where the largest eigenvalues λ_1 and λ_3 are given in Equations 13a and 13b.

Further approximations can be obtained if the population size N is very large and thus s is very small. In this case, the three-gene coalescence probability $q = s + O(s^2)$ as $s \to 0$ (Table 1), where the probability that three genes come from a single individual of the previous generation (multiple collisions) is ignored. Thus, the eigenvalues $\lambda_1 = 1 - s/2 + O(s^2)$ according to Equations 13a and 15a, and $\lambda_3 = 1 - 3s/2 + O(s^2)$ according to Equations 13b and 15b. This is consistent with the coalescent theory in a large random mating population where the effective population size N_e is given by $1/s$ and the coalescence rate of three genes is given by $3/(2N_e)$.

2^n-way RIL

RIL populations are a central type of breeding population from which many other types of populations can be derived with regard to the ancestral origin process along chromosomes. For example, one funnel in a CC population is an 8-way RIL population (Churchill *et al.* 2004), the maize nested associated mapping (NAM) population is a collection of independent 2-way RIL populations obtained by crossing a reference line to a set of diversity lines (Buckler *et al.* 2009), and the AMPRIL population is a collection of six independent 4-way RILs (Huang *et al.* 2011). In the framework of multistage breeding populations, the breeding design of RILs is $L = N_F = 2^n$, $\mathcal{M}_F = \mathcal{M}_I =$ pairing, and $\mathcal{M}_{II} =$ selfing or sibling. The founders are assumed to be completely inbred. The number of intercross (pairing) generations $U = n - 1$ for selfing, $U = 0$ for 2-way sibling mating, and $U = n - 2$ for 2^n-way ($n \geq 2$)

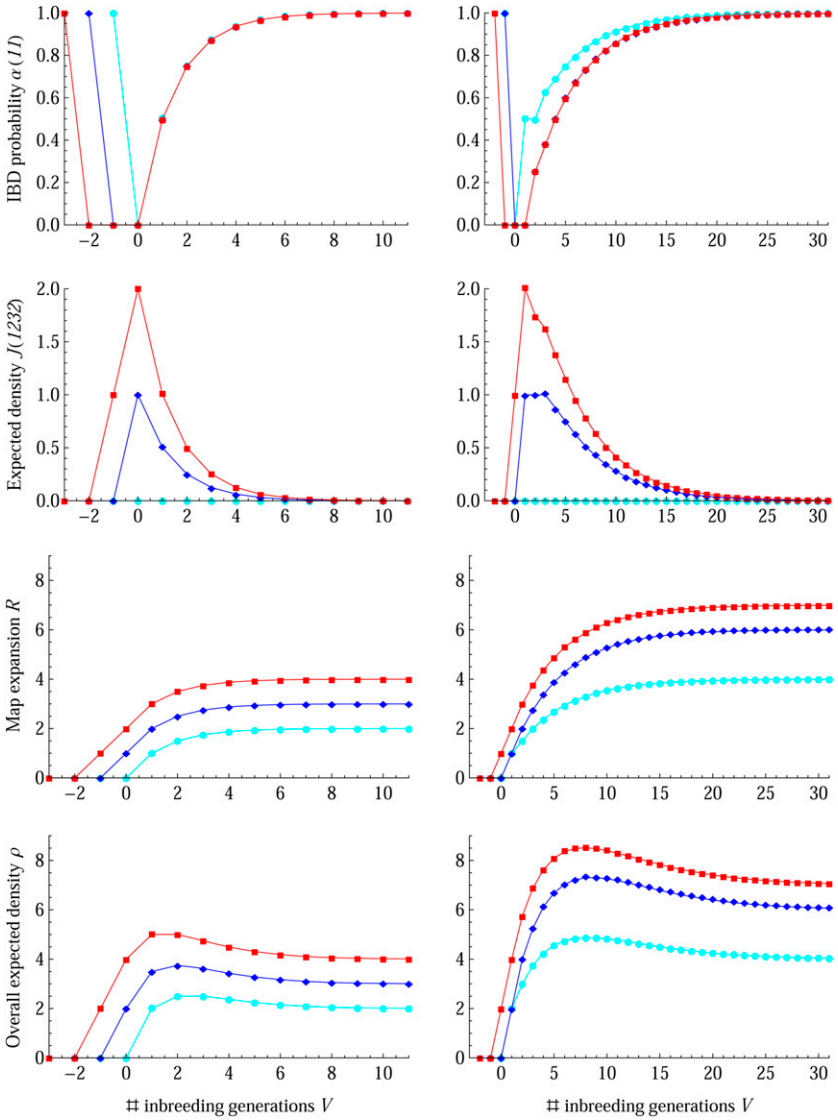

Figure 5 Results of 2^n-way RILs by selfing (left column) and sibling for autosomes (right column). The cyan circles, blue diamonds, and red rectangles denote the simulation results for n = 1, 2, and 3, respectively, and lines denote the theoretical results.

sibling mating. We focus on the inbreeding stage and refer to the subscript 0 in the initial conditions in Equations 14a–14e and Equations 16a–16e as generation $U + 1$.

Since inbreeding is completely avoided at the intercross stage of RILs, the initial conditions at generation $U + 1$ for the inbreeding stage can be obtained straightforwardly. It holds that $\alpha_{U+1}(12) = 1$, $J_{U+1}(1122) = 0$, and $J_{U+1}(1232) = R_{U+1} = U$ since each generation produces on average one junction per morgan in the case of no inbreeding. Putting these initial conditions into Equations 16a–16e and noting that the coalescence probability $s = 1$ for selfing at the inbreeding stage (Table 1), we obtain the results at the last generation $g = U + V + 1$ as shown in Table 2A for RILs by selfing.

For autosomes in RIL populations obtained by sibling mating, we need extra initial conditions. It holds that $K_{U+1}(1122) = 0$ and $K_{U+1}(1232) = U$. In addition, $\beta_{U+1}(12) = 1/2$, $\alpha_{U+1}(123) = 0$, and set $\beta_{U+1}(123) = 0$ for 2-way sibling mating; $\beta_{U+1}(12) = 1$ and $\alpha_{U+1}(123) = \beta_{U+1}(123) = 1$ for 2^n-way ($n \geq 2$) sibling mating. Putting all these initial conditions into Equations 14a–14e and noting that the coalescence probability $s = 1/2$ for sibling at the inbreeding stage (Table 1), we obtain the results at the last generation $g = U + V + 1$ as shown in Table 2, B and C.

Figure 5 shows that the closed-form solutions in Table 2 fit very well with the forward simulation results for two-, four-, and eight-way RILs by selfing or sibling. The differences between analytic and simulation results are small; see the left column of Figure 6 for the case of eight-way RILs by sibling mating; they may be due to the sampling error in a limited number of simulation replicates (10^4), but also due to the Markov approximation of ancestral origin processes. In contrast to the monotonic increasing of the map expansion R, a mode exists for the expected density $J(1232)$ and the overall expected density ρ, since the survival rate of old junctions remains the same and

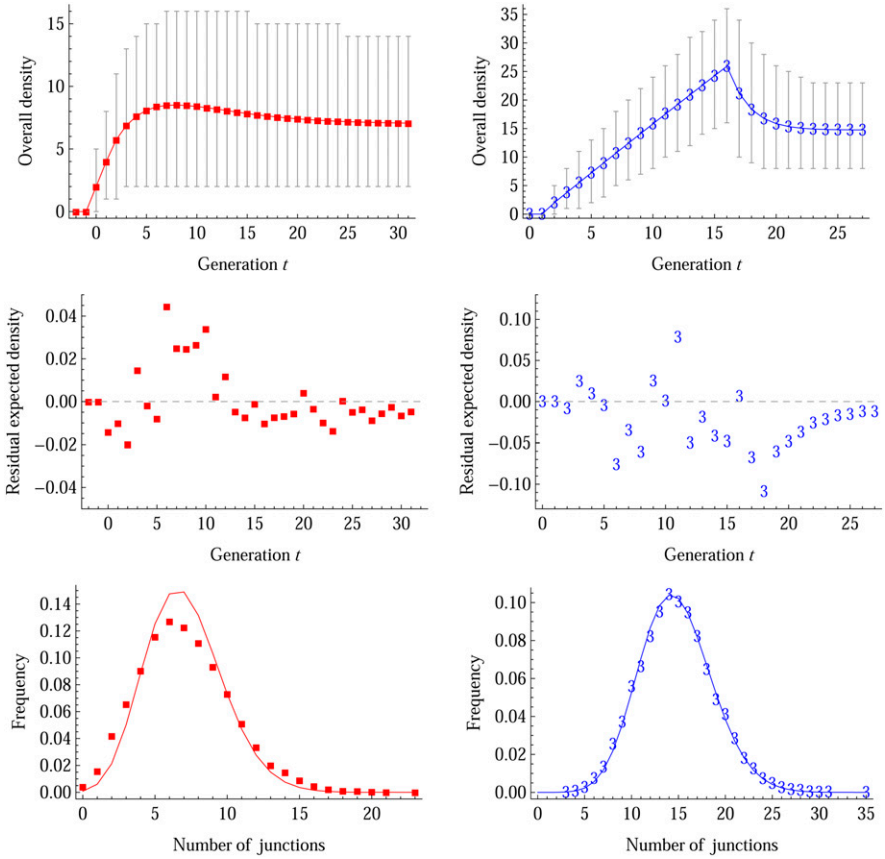

Figure 6 Simulation evaluations on the distribution of overall junction density. The left column shows the results for eight-way RILs by sibling mating, and the right column shows those for the MAGIC population with N_I = 100 and $\mathcal{M}_I$ = (3) RM1-E. In the top row, the solid lines are the theoretical expected densities, the plot markers (red dots and blue "3") are the means of the simulation results, and the error bars refer to the intervals between the 2.5% and 97.5% quantiles derived from 10^4 simulation replicates. Note that the error bar shows the variance of the overall junction density, but not the variance of the mean overall junction density (ρ). In the middle row, the residual expected densities refer to the simulated expectations subtracted by the theoretical values. In the bottom row, the solid lines refer to the theoretical Poisson distributions for the number of junctions within 1 M in length at the last generation, and the plot markers show the simulated values.

the gain rate of new junctions decreases when the population is getting more inbred, as shown in recurrence Equation 8b.

The map expansions R for 2^n-way ($n \geq 1$) RILs by selfing or sibling on autosomes, shown in Table 2, equal those given by Broman (2012a), although time origins are different. The AMPRIL population is a special RIL by selfing with $n = 2$ and $V = 3$, producing heterogeneous inbred lines (Huang *et al.* 2011). The overall expected density of this population at the last generation has been calculated to be $\rho = 3.625$ by using the inheritance vectors for the breeding pedigree, which is consistent with our results in Table 2A.

To guide the design of RIL populations in optimizing QTL map resolution, we calculate the three largest overall expected junction densities ρ and the corresponding inbreeding generations V according to the analytic expressions in Table 2. As shown in Table S2, for the 4-way RIL by selfing in the AMPRIL population, a larger overall expected density $\rho = 3.75$ would have been obtained if we reduce one generation of selfing ($V = 2$). In short, the F_3 population has largest ρ for 2-way RILs by selfing and the F_4 population for 4- or 8-way RILs by selfing; whereas for 2^n-way ($1 \leq n \leq 5$) RILs by sibling mating the F_9 population has largest ρ.

NIL

We can also derive the results for a biparental NIL population, although it does not fit in our framework. The two homologous chromosomes in a NIL population are no longer symmetric, and we need five independent expected junction densities. Suppose that the hybrid in each generation backcrosses with the fully inbred father parent, and thus there are no junctions on the paternally derived chromosome so that $J(1122) = J(1213) = J(1211) = 0$. The non-IBD probabilities in a biparental NIL population are the same as those for a two-way RIL by selfing, and the map expansion on the maternally derived chromosome of the hybrid is thus given by $R_g = 2[1 - (1/2)^V]$ at the last generation $g = U + V + 1$ with $U = 0$ (see Table 2) since Equation 7 still holds. It holds that $J_g(1232) = 0$ and $J_g(1222) = J_g(1121) = R_g/2$.

MAGIC populations

The MAGIC population is an advanced breeding population. It generalizes the advanced intercross lines (AILs) (Darvasi and Soller 1995) and the heterogeneous stock (HS) population (Mott *et al.* 2000) by attaching an inbreeding stage to produce (nearly) completely inbred lines. MAGIC can also be regarded as a RIL population with a modified intercross mating scheme, $\mathcal{M}_I$, from pairing to random mating. In the following, we apply our model to study the breeding design of MAGIC populations by varying the number N_F of inbred founders or the intercross mating scheme $\mathcal{M}_I$, in terms of the map expansion R and the overall expected junction density ρ that are used as measures of map resolution in QTL mapping populations.

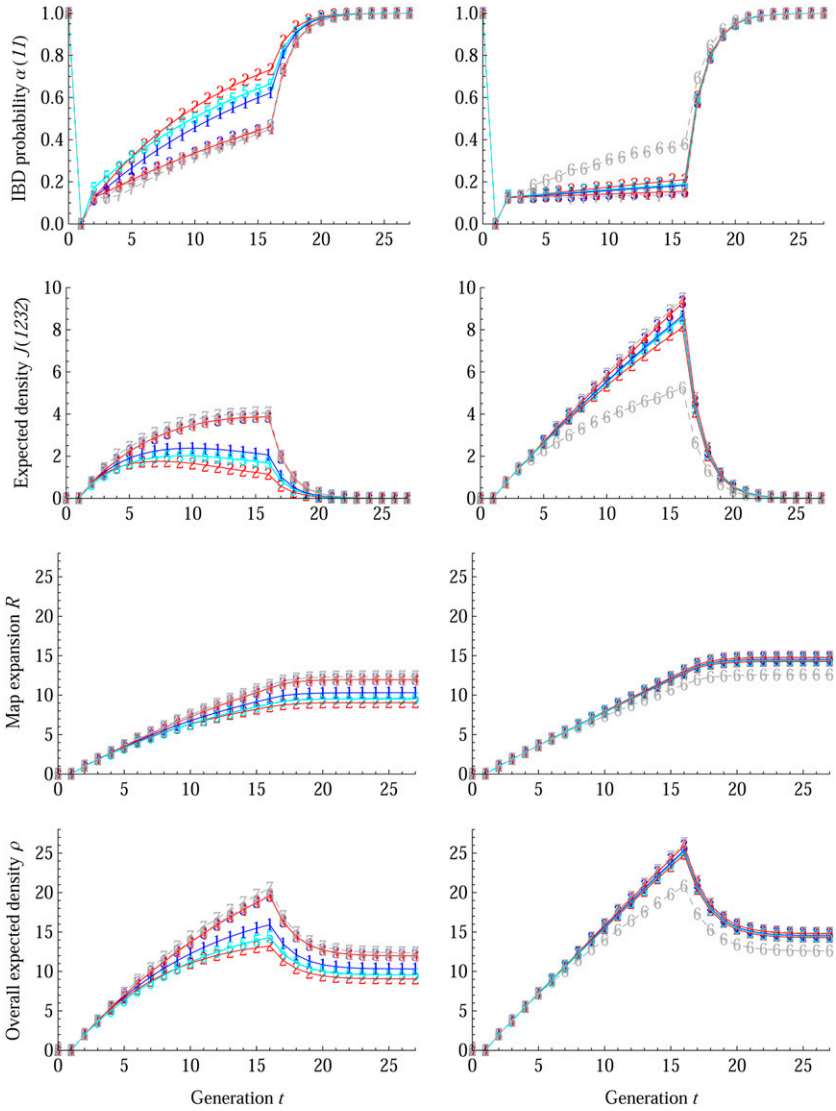

Figure 7 Breeding designs on the intercross mating scheme $\mathcal{M}_{\text{I}}$ in MAGIC populations with $N_{\text{F}} = 8$, $\mathcal{M}_{\text{F}}$ = RM1-NE, and $\mathcal{M}_{\text{II}}$ = selfing. The intercross population size $N_{\text{I}} = 8$ in the left column and $N_{\text{I}} = 100$ in the right column. The simulation results are denoted by integer markers for $\mathcal{M}_{\text{I}}$ = (1) RM1-NE, (2) RM2-NE, (3) RM1-E, (4) RM2-E, (5) WF-NE, (6) CPM-E, and (7) MAI-E, respectively. The solid lines represent the theoretical results for the random intercross schemes, and dashed lines connect simulation results for the regular schemes (6) CPM-E and (7) MAI-E to guide one's eyes. The blue color is for (1) RM1-NE and (3) RM1-E, red is for (2) RM2-NE and (4) RM2-E, cyan is for (5) WF-NE, and gray is for (6) CPM-E and (7) MAI-E.

We first study the effects of the intercross mating scheme $\mathcal{M}_{\text{I}}$ by both the forward simulations and the theoretical recurrence relations described in the *Methods* section. In total, seven intercross mating schemes $\mathcal{M}_{\text{I}}$ are included: (1) RM1-NE, (2) RM2-NE, (3) RM1-E, (4) RM2-E, (5) WF-NE, (6) CPM-E, and (7) MAI-E. There are no theoretical results for the two regular mating schemes (CPM-E and MAI-E), since our model does not apply to them. We set $\mathcal{M}_{\text{II}}$ = selfing for the inbreeding stage, since it is feasible for MAGIC populations used in *Arabidopsis* and many important crops. For the mixing stage, we set $N_{\text{F}} = 8$, $\mathcal{M}_{\text{F}}$ = RM1-NE, and $N_{\text{I}} = 8$ or 100 for each of two sets of simulations. We use RM1-NE as the mixing random mating scheme instead of commonly used diallel crosses, so that the intercross population size N_{I} can be chosen arbitrarily (Table 1).

Figure 7 shows the effects of the intercross mating scheme $\mathcal{M}_{\text{I}}$ on the IBD probability $\alpha(11)$, the expected density $J(1232)$, the map expansion R, and the overall expected junction density ρ. Their sharp changes indicate the transition from the intercross stage to the inbreeding stage in the breeding design. Theoretical results fit the simulations very well, and the differences are negligible; see the right column of Figure 6 for the MAGIC population with $N_{\text{I}} = 100$ and $\mathcal{M}_{\text{I}}$ = (3) RM1-E. The effects of intercross scheme $\mathcal{M}_{\text{I}}$ are small in the beginning, and we thus consider the effects only after 10 generations. As shown in the left column of Figure 7 for $N_{\text{I}} = 8$, the ranking of intercross scheme $\mathcal{M}_{\text{I}}$ on R and ρ is RM2-NE < WF-NE < RM1-NE < RM1-E = RM2-E < CPM-E < MAI-E. The right column of Figure 7 show similar ranking for $N_{\text{I}} = 100$: CPM-E ≪ RM2-NE < WF-NE < RM1-NE < RM1-E = RM2-E < MAI-E, except that CPM-E is far smaller and all other mating schemes are similar. The ranking of intercross scheme $\mathcal{M}_{\text{I}}$ on the IBD probability $\alpha(11)$ is inversed, which is reasonable since the map expansion is an accumulation of the non-IBD probability $\alpha(12)$ (see Equation 7).

The results of Figure 7 indicate that random mating schemes with equal contributions are better than those with nonequal contributions, and MAI-E is slightly better. They are consistent with those of the simulation studies of Rockman and Kruglyak (2008) on recombinant inbred AIL populations, where there are two inbred founders. However, the differentiations of intercross

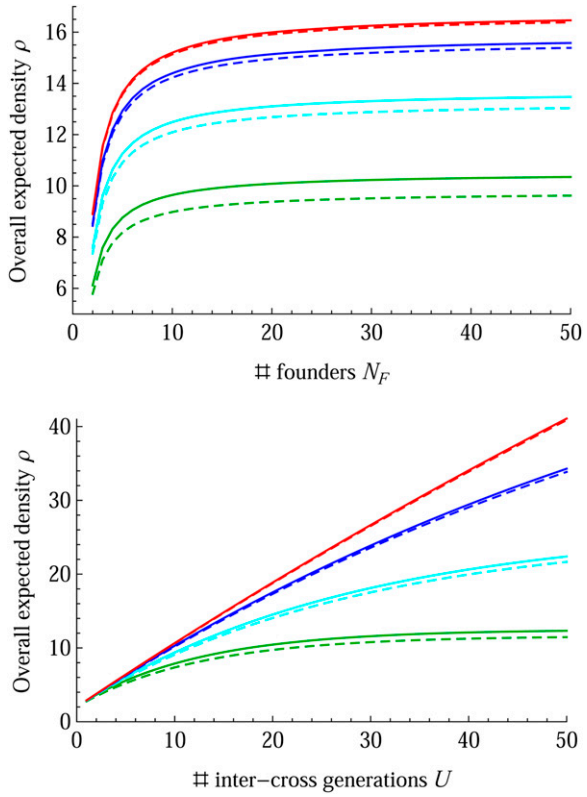

Figure 8 Breeding designs for the number of founders N_F and the number of intercross generations U in MAGIC populations. The overall expected density ρ_g is at the last generation $g = U + V + 1$. The basic design is $\mathcal{M}_F$ = RM1-NE, $\mathcal{M}_I$ = RM1-E, $\mathcal{M}_{II}$ = selfing, and $V = 6$. Top, $U = 15$; bottom, $N_F = 8$. The line colors green, cyan, blue, and red denote the results for $N_I = 4$, 8, 20, and 50, respectively. The solid lines represent the results from the recurrence relations, and the dashed lines show those from the approximation of Equation 18.

scheme $\mathcal{M}_I$ (except CPM-E) diminish with increasing intercross population size. Thus, we derive below closed-form solutions for the map expansion R and the overall density ρ in MAGIC populations, assuming that the intercross population size N_I is large and that $\mathcal{M}_{II}$ = selfing at the inbreeding stage. We denote by s_F (or s_I) the constant coalescence probabilities at the mixing (or intercross) stage.

The closed-form solutions of R and ρ can be obtained by applying Equation 3 and Equations 16c and 16d to the intercross stage with the initial conditions at generation 2 and then to the selfing inbreeding stage with the initial conditionals at generation $U + 1$. Here we assume that the intercross population size N_I is large so that $\alpha_2(12) \approx \beta_2(12)$ and Equations 16c and 16d are good approximations for the nonselfing intercross mating scheme $\mathcal{M}_I$. In the founder population, $\alpha_0(12) = 0$, $\beta_0(12) = 1$, and $J_0(1122) = K_0(1122) = R_0 = 0$. The initial conditions at generation 2 can be obtained: $\alpha_2(12) \approx s_I/2 + (1 - s_I)(1 - s_F)$, $R_2 = 1$, and $J_2(1122) = 0$ according to the recurrence relations for a nonselfing mixing mating scheme $\mathcal{M}_F$. We obtain for the last generation $g = U + V + 1$,

$$R_g = 1 + \frac{\alpha_2(12)}{1-\lambda_1}\left[1 - (\lambda_1)^{U-1}\right] + 2\alpha_2(12)(\lambda_1)^{U-1}\left[1 - \left(\frac{1}{2}\right)^V\right], \tag{17}$$

$$\rho_g = 1 + (\lambda_1)^{U-1}\left(\frac{1}{2}\right)^V + \frac{\alpha_2(12)}{1-\lambda_1}\left[1 - \left(1 - \frac{1-\lambda_1}{\lambda_1}(U-1)\left(\frac{1}{2}\right)^V\right)(\lambda_1)^{U-1}\right] + 2\alpha_2(12)(\lambda_1)^{U-1}\left[1 + (V-1)\left(\frac{1}{2}\right)^V\right], \tag{18}$$

where $U \geq 1$, and the eigenvalue λ_1 of the intercross stage is given by Equation 13a for nonselfing intercross mating $\mathcal{M}_I$ and otherwise by Equation 15a. Both R and ρ converge to those of 2^n-way ($n \geq 2$) RILs by selfing when $\alpha_2(12) = 1$ and $\lambda_1 \to 1$ (Table 1).

The expected densities of R and ρ in Equations 17 and 18 show that they are linearly related to $\alpha_2(12)$ and thus approximately linearly related to $1/N_F$, the inverse of the number of founders according to the coalescence probability s_F in Table 1, and that they are also asymptotically linearly related to the number U of intercross generations when the intercross population size N_I increases and thus $\lambda_1 \to 1$. Figure 8 shows that ρ becomes flat when $N_F > \sim 10$ and that the approximation of ρ in Equation 18 slightly underestimates those obtained from the recurrence relations, but it gets very accurate as the intercross population size N_I increases up to ~ 50.

Discussion

We have presented a general framework for modeling ancestral origin processes in a wide range of diploid breeding populations such as RILs, AILs, HSs, and MAGICs. For a new type of breeding population, we may apply the recurrence relations or deduce closed-form solutions if the design is stage-wise. The model framework may also be applied to natural populations if a recently founded population exists. In this scenario, the model parameters such as the coalescence probabilities or the effective population size are usually unknown, and they have to be estimated jointly with the ancestral origins from the genetic marker data.

The closed-form solutions of the expected junction densities are obtained for 2^n-way RILs by selfing or sibling for any natural number $n \geq 1$. From these expected densities, the rate matrix of the continuous time Markov chain of ancestral origin processes can be deduced and then the diplotype probabilities. Broman (2012a) extended the approach of Haldane and Waddington (1931) to 4- and 8-way RIL populations from sibling mating, but that approach does not lead to explicit expressions for two-locus diplotype probabilities.

One key assumption of our approach is the symmetry of founders in breeding populations. It helps to reduce model complexity greatly, so that our model can be applied to an arbitrary number of founders, whereas the complexity of the approach by Haldane and Waddington (1931) and Broman (2012a) increases very fast with the number of founders. Meanwhile, the approximation does not affect the results on junction densities where only changes of founder origins matter. The assumption is valid for MAGIC populations with random mating schemes and for 2^n-way ($n \geq 1$) RILs by selfing, but not valid for 2^n-way ($n \geq 2$) RILs by sibling mating due to the initial exclusive pairwise mating. However, this violation is not critical since individual samples are collected at the last generation and their ancestral genomes have been well mixed by many generations of random chromosomal segregations during inbreeding.

The second key assumption is the Markov property of ancestral origin processes along chromosomes. Therefore our model reduces to the IBD model of Stam (1980), where IBD and non-IBD tracts are exponentially distributed. However, even under the model of the sequential Markov coalescence (McVean and Cardin 2005; Marjoram and Wall 2006), the IBD tract length is not exponentially distributed, because the transition rate depends on the total branch length of the local tree, that is, the coalescent time in the case of two chromosomes. The nonexponential distribution for the length of IBD tracts has been modeled by Martin and Hospital (2011) in two-way RILs by sibling mating and by Chapman and Thompson (2003) in random mating populations, and their results show that the deviations from nonexponential distributions are acceptable, particularly for large populations.

The deviation from the Markov property is reflected in the variances of junction densities. The occurrence of junctions along two homologous chromosomes is an inhomogeneous process according to the continuous time Markov model. However, for the case of a nearly complete inbred individual at the last generation, the distribution of the overall junction density follows approximately a Poisson distribution with mean ρ. As shown in Figure 6 for eight-way RILs by sibling mating, the simulated variance ($\sim$10) of the overall junction density is larger than the theoretical variance ($\sim$7); whereas for the MAGIC population with N_I = 100 and $\mathcal{M}_I$ = (3) RM1-E, the theoretical Poisson distribution fits very well with the simulated distribution. The goodness of fit depends very little on the intercross random mating scheme, but it becomes slightly worse for small intercross population size N_I = 8.

Finally, the breeding design assumes a single random mating population with variable size and no population structure. In contrast to the above two assumptions, this assumption does affect the expected junction densities. The breeding mating schemes of selfing and sibling and the mixing mating schemes of diallel crosses are regarded as special kinds of random mating. Essentially, a pair of individuals in the same generation is assumed to be statistically equivalent in terms of ancestral origins. For regular mating schemes such as CPM or subdivided populations, a set of recurrence relations is needed to account for different distances between two individuals, as shown by Kimura and Crow (1963) in calculating two-gene IBD probabilities.

The approximation of random mating implies the lack of natural selection since the founder population. Our model does not apply to those parts of genomes in breeding populations that are under artificial or natural selection. Still, even here we can use our model as a null model to investigate the strength of selection. Furthermore, we can try to use our model for describing parts of the breeding process like the inbreeding stage.

Liu *et al.* (2010) described a hidden Markov model (HMM) for ancestral inference in complex pedigrees with inbreeding from genetic marker data, where the inbreeding model is integrated into the Lander–Green algorithm. Their prior inbreeding model is specially built for sibling mating, and it is a discrete time Markov process. They model the two-locus diplotype probabilities $D(abcd)$ between neighbor markers under an assumption of small intermarker distance ($<$0.001 M). Similarly, Liu *et al.* (2010) reduced the diplotype probabilities into three basic probabilities, where the diplotype probability $D(1232)$ was calculated through the recurrence relations of the probabilities of three and four distinct genes among two siblings.

An HMM is under development for reconstructing ancestral origins from marker data, by using the present model of ancestral origin processes as the prior distribution. Then, we will be able to evaluate our general approach with both the specially designed model of Liu *et al.* (2010) and a relatively simple HMM approach such as that in R/happy (Mott *et al.* 2000) that does not account for the joint pattern of recombination breakpoints in two homologous chromosomes.

Acknowledgments

The authors have no competing financial interests. This research was supported by the Stichting Technische Wetenschappen (STW) - Technology Foundation, which is part of the Nederlandse Organisatie voor Wetenschappelijk Onderzoek - Netherlands Organisation for Scientific Research, and is partly funded by the Ministry of Economic Affairs, under grant no. STW-Rijk Zwaan project 12425.

Literature Cited

Bennett, J. H., 1953 Junctions in inbreeding. Genetica 26: 392–406.

Bennett, J. H., 1954 The distribution of heterogeneity upon inbreeding. J. R. Stat. Soc. Ser. B Stat. Methodol. 16: 88–99.

Boucher, W., and T. Nagylaki, 1988 Regular systems of inbreeding. J. Math. Biol. 26: 121–142.

Broman, K., 2005 The genomes of recombinant inbred lines. Genetics 169: 1133–1146.

Broman, K. W., 2012a Genotype probabilities at intermediate generations in the construction of recombinant inbred lines. Genetics 190: 403–412.

Broman, K. W., 2012b Haplotype probabilities in advanced intercross populations. G3 2: 199–202.

Buckler, E. S., J. B. Holland, P. J. Bradbury, C. B. Acharya, P. J. Brown *et al.*, 2009 The genetic architecture of maize flowering time. Science 325: 714–718.

Cavanagh, C., M. Morell, I. Mackay, and W. Powell, 2008 From mutations to magic: resources for gene discovery, validation and delivery in crop plants. Curr. Opin. Plant Biol. 11: 215–221.

Chapman, N., and E. Thompson, 2003 A model for the length of tracts of identity by descent in finite random mating populations. Theor. Popul. Biol. 64: 141–150.

Churchill, G., D. Airey, H. Allayee, J. Angel, A. Attie *et al.*, 2004 The collaborative cross, a community resource for the genetic analysis of complex traits. Nat. Genet. 36: 1133–1137.

Cockerham, C., 1971 Higher order probability functions of identity of alleles by descent. Genetics 69: 235–246.

Darvasi, A., and M. Soller, 1995 Advanced intercross lines, an experimental population for fine genetic-mapping. Genetics 141: 1199–1207.

Fisher, R., 1949 *The Theory of Inbreeding*. Oliver & Boyd, London.

Fisher, R., 1954 A fuller theory of junctions in inbreeding. Heredity 8: 187–197.

Haldane, J., and C. Waddington, 1931 Inbreeding and linkage. Genetics 16: 357–374.

Huang, X., M.-J. Paulo, M. Boer, S. Effgen, P. Keizer *et al.*, 2011 Analysis of natural allelic variation in *Arabidopsis* using a multiparent recombinant inbred line population. Proc. Natl. Acad. Sci. USA 108: 4488–4493.

Johannes, F., and M. Colome-Tatche, 2011 Quantitative epigenetics through epigenomic perturbation of isogenic lines. Genetics 188: 215–227.

Kimura, M., and J. F. Crow, 1963 On maximum avoidance of inbreeding. Genet. Res. 4: 399–415.

Kover, P. X., W. Valdar, J. Trakalo, N. Scarcelli, I. M. Ehrenreich *et al.*, 2009 A multiparent advanced generation inter-cross to fine-map quantitative traits in *Arabidopsis thaliana*. PLoS Genet. 5: e1000551.

Liu, E. Y., Q. Zhang, L. McMillan, F. Pardo-Manuel de Villena, and W. Wang, 2010 Efficient genome ancestry inference in complex pedigrees with inbreeding. Bioinformatics 26: i199–i207.

MaCleod, A. K., C. S. Haley, and J. A. Woolliams, 2005 Marker densities and the mapping of ancestral junctions. Genet. Res. 85: 69–79.

Marjoram, P., and J. D. Wall, 2006 Fast "coalescent" simulation. BMC Genet. 7: 16.

Martin, O. C., and F. Hospital, 2011 Distribution of parental genome blocks in recombinant inbred lines. Genetics 189: 645–654.

McVean, G., and N. Cardin, 2005 Approximating the coalescent with recombination. Philos. Trans. R. Soc. Lond. B Biol. Sci. 360: 1387–1393.

Mott, R., C. Talbot, M. Turri, A. Collins, and J. Flint, 2000 A method for fine mapping quantitative trait loci in outbred animal stocks. Proc. Natl. Acad. Sci. USA 97: 12649–12654.

Nadot, R., and G. Vayssiex, 1973 Algorithme du calcul des coefficients d'identite. Biometrics 29: 347–359.

Norris, J. R., 1997 *Markov Chains*. Cambridge University Press, Cambridge, UK/London/New York.

Rockman, M. V., and L. Kruglyak, 2008 Breeding designs for recombinant inbred advanced intercross lines. Genetics 179: 1069–1078.

Stam, P., 1980 The distribution of the fraction of the genome identical by descent in finite random mating populations. Genet. Res. 35: 131–155.

Teuscher, F., and K. W. Broman, 2007 Haplotype probabilities for multiple-strain recombinant inbred lines. Genetics 175: 1267–1274.

Valdar, W., J. Flint, and R. Mott, 2003 QTL fine-mapping with recombinant-bred heterogeneous stocks and in vitro heterogeneous stocks. Mamm. Genome 14: 830–838.

Voight, B. F., and J. K. Pritchard, 2005 Confounding from cryptic relatedness in case-control association studies. PLoS Genet. 1: e32.

Weller, J., and M. Soller, 2004 An analytical formula to estimate confidence interval of qtl location with a saturated genetic map as a function of experimental design. Theor. Appl. Genet. 109: 1224–1229.

Winkler, C., N. Jensen, M. Cooper, D. Podlich, and O. Smith, 2003 On the determination of recombination rates in intermated recombinant inbred populations. Genetics 164: 741–745.

Wright, S., 1921 Systems of mating. II. The effects of inbreeding on the genetic composition of a population. Genetics 6: 124–143.

Communicating editor: B. S. Yandell

GENETICS

Supporting Information
http://www.genetics.org/lookup/suppl/doi:10.1534/genetics.114.163006/-/DC1

A General Modeling Framework for Genome Ancestral Origins in Multiparental Populations

Chaozhi Zheng, Martin P. Boer, and Fred A. van Eeuwijk

DOI: 10.1534/genetics.114.163006

File S1

Supplementary Materials

S1 Expressions of the constant coefficients

The coefficients C_1 and C_2 in equation (14a) are determined by the initial conditions $\alpha_0(12) = C_1 + C_2$ and $\alpha_1(12) = \beta_0(12) = C_1\lambda_1 + C_2\lambda_2$. Thus we have

$$C_1 = \frac{\beta_0(12) - \alpha_0(12)\lambda_2}{\lambda_1 - \lambda_2}, \tag{S1.1a}$$

$$C_2 = -\frac{\beta_0(12) - \alpha_0(12)\lambda_1}{\lambda_1 - \lambda_2}. \tag{S1.1b}$$

The coefficients C_3 and C_4 in equation (14b) are determined by the initial conditions $\alpha_0(123) = C_3 + C_4$ and $\alpha_1(123) = C_3\lambda_3 + C_4\lambda_4$. According to equation (5a) it holds $\alpha_1(123) = s\alpha_0(123) + (1-2s)\beta_0(123)$, and thus we have

$$C_3 = \frac{(1-2s)\beta_0(123) + (s-\lambda_4)\alpha_0(123)}{\lambda_3 - \lambda_4}, \tag{S1.2a}$$

$$C_4 = \alpha_0(123) - C_3 \tag{S1.2b}$$

where we set $C_3 = \alpha_0(123)$ and $C_4 = 0$ for the case of $\lambda_3 = \lambda_4$.

According to the recurrence equations (10a, 10b), we have

$$J_t(1122) = (1-s)J_{t-1}(1122) + \frac{s}{2}J_{t-2}(1122) + \frac{s}{2}R_{t-2}. \tag{S1.3}$$

Substituting the equations (14c, 14d) into the above recurrence relation and noting that $\lambda_{1,2}^2 - (1-s)\lambda_{1,2} - s/2 = 0$, we have

$$C_6 = -\frac{C_1}{1 + s - 2\lambda_1 s}, \tag{S1.4}$$

$$C_8 = -\frac{C_2}{1 + s - 2\lambda_2 s}. \tag{S1.5}$$

Let $C_0 = [R_0 + C_1/(1-\lambda_1) + C_2/(1-\lambda_2)]$, from the initial condition $J_0(1122) = C_0 + C_5 + C_7$, $J_1(1122) = K_0(1122) = C_0 + (C_5 + C_6)\lambda_1 + (C_7 + C_8)\lambda_2$, the expressions for C_5 and C_7

are given by

$$C_5 = \frac{K_0(1122) - C_0 - C_6\lambda_1 - C_8\lambda_2 - \lambda_2 \left[J_0(1122) - C_0\right]}{\lambda_1 - \lambda_2}, \tag{S1.6}$$

$$C_7 = J_0(1122) - C_5 - C_0. \tag{S1.7}$$

We can obtain expressions for $C_9, ...C_{12}$ similarly. According to the recurrence equations (8a, 8b), we have

$$J_t(1232) = (1-s)J_{t-1}(1232) + \frac{s}{2}J_{t-2}(1213) + \alpha_{t-1}(123). \tag{S1.8}$$

Substituting the equations (14b, 14e) into the above recurrence relation, we have

$$C_{11} = \frac{C_3\lambda_3}{\lambda_3^2 - (1-s)\lambda_3 - s/2}, \tag{S1.9}$$

$$C_{12} = \frac{C_4\lambda_4}{\lambda_4^2 - (1-s)\lambda_4 - s/2}. \tag{S1.10}$$

From the inital conditions $J_0(1232) = C_9 + C_{10} + C_{11} + C_{12}$ and $J_1(1232) = K_0(1232) + \alpha_0(123) = C_9\lambda_1 + C_{10}\lambda_2 + C_{11}\lambda_3 + C_{12}\lambda_4$, we have

$$C_9 = \frac{K_0(1232) + \alpha_0(123) - C_{11}\lambda_3 - C_{12}\lambda_4 - \lambda_2 \left[J_0(1232) - C_{11} - C_{12}\right]}{\lambda_1 - \lambda_2} \tag{S1.11}$$

$$C_{10} = J_0(1232) - C_9 - C_{11} - C_{12}. \tag{S1.12}$$

Table S1 List of symbols and their brief explanations.

Category	Symbol	Explanation
Two-gene	(ab)	Two-gene IBD configurations include (11) and (12)
	$\alpha_t(ab)$	Within-individual probability of configuration (ab) in generation *t*
	$\beta_t(ab)$	Between-individual probability of configuration (ab) in generation *t*
	$\alpha_t(11)$	Within-individual two-gene IBD probability in generation *t*
	$\alpha_t(12)$	Within-individual two-gene non-IBD probability in generation *t*
	s_t	Two-gene coalescence probability that both come from a single individual of the previous generation $t-1$
Three-gene	(abc)	Three-gene IBD configurations include (111), (112), (121), (122), (123)
	$\alpha_t(abc)$	Probability of configuration (abc) in generation *t,* given that genes a and c are in a single individual and gene b in another
	$\beta_t(abc)$	Probability of configuration (abc) in generation *t*, given that the three genes are in three distinct individuals
	$\alpha_t(123)$	Non-IBD probability of the three genes
	$\alpha_t(122)$	Probability that the genes a and b are non-IBD and genes b and c are IBD
	$\alpha_t(1\_2)$	Marginal non-IBD probability between genes a and c
	q_t	Three-gene coalescence probability that one particular gene comes from one individual and other two genes come from another individual of the previous generation $t-1$.
Four-gene	$(abcd)$	Four-gene IBD configurations include the 15 configurations shown in Table 1
	$D(abcd)$	Two-locus probability of configuration $(abcd)$
	$J_t(abcd)$	Within-individual expected junction density of type $(abcd)$ in generation *t*. The seven junction types are shown in Table 1
	$K_t(abcd)$	Between-individual expected junction density of type $(abcd)$ in generation *t*
Breeding design	L	Number of distinct founder genome labels (FGL)
	U	Number of intercross generations
	V	Number of inbreeding generations
	N_t	Population size in generation *t*
	N_F	Constant size of founder population, and N_F=*L* if founders are fully inbred
	N_I	Constant size of intercross populations
	N_{II}	Constant size of inbred populations. $N_{II}=1$ if $\mathcal{M}_{II}=\text{Selfing}$, and $N_{II}=2$ if $\mathcal{M}_{II}=\text{Sibling}$
	$\mathcal{M}_t$	Mating scheme from the generation *t* to the next generation.
	$\mathcal{M}_F$	Constant mating scheme from the founder population to the F_1 population, $\mathcal{M}_F=\mathcal{M}_0$
	$\mathcal{M}_I$	Constant mating scheme in the intercross stage, $\mathcal{M}_I=\mathcal{M}_1=\cdots=\mathcal{M}_U$
	$\mathcal{M}_{II}$	Constant mating scheme in the inbreeding stage, $\mathcal{M}_{II}=\mathcal{M}_{U+1}=\cdots=\mathcal{M}_{U+V}$
Map resolution	R	Map expansion, the expected junction density (per Morgan) on one chromosome
	ρ	Overall expected junction density, the expected junction density (per Morgan) on two homologous chromosomes

Table S2 The three largest overall expected junction densities ρ for 2^n-way RIL on autosomes at the last generation $g = U + V + 1$.

Scheme	n	U	(ρ, V)		
Selfing	1	0	(2.5, 2)	(2.5, 3)	(2.375, 4)
	2	1	(3.75, 2)	(3.625, 3)	(3.5, 1)
	3	2	(5, 1)	(5, 2)	(4.75, 3)
	4	3	(6.5, 1)	(6.25, 2)	(6, 0)
	5	4	(8, 0)	(8, 1)	(7.5, 2)
	6	5	(10, 0)	(9.5, 1)	(8.75, 2)
Sibling	1	0	(4.875, 8)	(4.863, 9)	(4.844, 7)
mating	2	0	(7.301, 8)	(7.297, 7)	(7.256, 9)
	3	1	(8.512, 7)	(8.484, 6)	(8.475, 8)
	4	2	(9.75, 6)	(9.727, 7)	(9.688, 5)
	5	3	(11.016, 5)	(11.016, 6)	(10. 941, 7)
	6	4	(12.344, 5)	(12.312, 4)	(12.281, 6)